

Directional Growth of Ultra-long CsPbBr₃ Perovskite Nanowires for High Performance Photodetectors

Muhammad Shoaib, Xuehong Zhang, Xiaoxia Wang, Hong Zhou, Tao Xu, Xiao Wang, Xuelu Hu, Huawei Liu, Xiaopeng Fan, Weihao Zheng, Tiefeng Yang, Shuzhen Yang, Qinglin Zhang, Xiaoli Zhu, Litao Sun, and Anlian Pan

J. Am. Chem. Soc., **Just Accepted Manuscript** • DOI: 10.1021/jacs.7b08818 • Publication Date (Web): 23 Oct 2017

Downloaded from <http://pubs.acs.org> on October 24, 2017

Just Accepted

“Just Accepted” manuscripts have been peer-reviewed and accepted for publication. They are posted online prior to technical editing, formatting for publication and author proofing. The American Chemical Society provides “Just Accepted” as a free service to the research community to expedite the dissemination of scientific material as soon as possible after acceptance. “Just Accepted” manuscripts appear in full in PDF format accompanied by an HTML abstract. “Just Accepted” manuscripts have been fully peer reviewed, but should not be considered the official version of record. They are accessible to all readers and citable by the Digital Object Identifier (DOI®). “Just Accepted” is an optional service offered to authors. Therefore, the “Just Accepted” Web site may not include all articles that will be published in the journal. After a manuscript is technically edited and formatted, it will be removed from the “Just Accepted” Web site and published as an ASAP article. Note that technical editing may introduce minor changes to the manuscript text and/or graphics which could affect content, and all legal disclaimers and ethical guidelines that apply to the journal pertain. ACS cannot be held responsible for errors or consequences arising from the use of information contained in these “Just Accepted” manuscripts.



Directional Growth of Ultra-long CsPbBr₃ Perovskite Nanowires for High Performance Photodetectors

Muhammad Shoaib,^{†§} Xuehong Zhang,^{†§} Xiaoxia Wang,^{†§} Hong Zhou,[†] Tao Xu,[‡] Xiao Wang,[†] Xuelu Hu,[†] Huawei Liu,[†] Xiaopeng Fan,[†] Weihao Zheng,[†] Tiefeng Yang,[†] Shuzhen Yang,[†] Qinglin Zhang,[†] Xiaoli Zhu,[†] Litao Sun,[‡] Anlian Pan^{†*}

[†] Key Laboratory for Micro-Nano Physics and Technology of Hunan Province, State Key Laboratory of Chemo/Biosensing and Chemometrics, and School of Physics and Electronic Science, Hunan University, Changsha, Hunan 410082, P. R. China

[‡]SEU-FEI Nano-Pico Center, Key Lab of MEMS of Ministry of Education, Southeast University, Nanjing 210096, P. R. China

Supporting Information Placeholder

ABSTRACT: Directional growth of ultra-long nanowires is of great significance for the practical application of large-scale optoelectronic integration. Here, we demonstrate the controlled growth of in-plane directional perovskite CsPbBr₃ nanowires, induced by graphoepitaxial effect on annealed M-plane sapphire substrates. The wires have a diameter of several hundred of nanometers, with their length reaching up to several millimeters. Microstructure characterization shows that the CsPbBr₃ nanowires are high-quality single crystals, with smooth surfaces and well-defined cross-section. The nanowires own very strong bandedge photoluminescence (PL) with a long PL lifetime of ~25 ns, and can realize high-quality optical waveguides. Photodetectors constructed on these individual nanowires exhibit excellent photoresponse with an ultra-high responsivity of 4400 A/W and a very fast response speed of 252 μs. This work presents an important step towards scalable growth of high quality perovskite nanowires, which will find more promising opportunities in constructing integrated nanophotonic and optoelectronic systems.

Inorganic semiconductor perovskite CsPbX₃ (X=Cl, Br, I) nanostructures have attracted tremendous attention for developing novel light emitting diodes, lasers, and photodetectors, due to their extraordinary optoelectronic properties.¹⁻⁷ Though CsPbX₃ quantum dots, nanoplates, and nanowires have been well realized by solution based methods,⁸⁻¹¹ the conventional chemical vapor deposition (CVD) method, that is generally exploited to grow high-quality electronic materials, may offer an alternative pathway to achieve high quality all-inorganic perovskite nanostructures. Many efforts have recently been devoted to realize the growth of perovskite CsPbX₃ nanostructures using the vapor route, including single crystalline nanoplatelets, nanowire networks, and nano/microrods.¹²⁻¹⁷

Large-scale growth or assembly of semiconductor nanowires with horizontal alignment on surfaces is highly desirable in future integrated devices.¹⁸⁻²⁰ In this regard, the growth of directional and ultra-long CsPbX₃ nanowires would be an important step in their integration into practical devices, but still remains challenging. Recently, ultra-long organic-inorganic perovskite wires were synthesized via template assisted solution methods.²¹ However, the solution growth of all-inorganic perovskites is difficult due to the lower solubility of inorganic perovskites and more complex Cs-Pb-X phase diagram.²² Graphoepitaxial effect assisted vapor growth has been well developed to realize the growth of horizontal and aligned semiconductor nanowires on sapphire substrates with well aligned nanosteps or grooves, which can provide a max-

imum interface area between the substrate and the nanowires, resulting in the directional and continuous growth of the nanowires.²³⁻²⁷

Here, we report, for the first time, the successful vapor growth of ultra-long directional CsPbBr₃ perovskite nanowires using the graphoepitaxial effect on annealed M-plane sapphire substrates. The wires are well aligned along the groove direction of the substrate, with the length up to several millimeters, demonstrating the longest CsPbX₃ nanowires reported so far. Microstructure characterizations demonstrate the high quality single-crystal nature of the achieved wires, which was further revealed by the exhibited strong light emission and excellent optical waveguiding. High performance photodetectors have been achieved based on these individual CsPbBr₃ nanowires, which own a responsivity of 4400 A/W and a response speed of 252 μs, a lot higher than all the previously reported photodetectors on single halide perovskite nano/microstructures.²⁸⁻³⁶ This study makes an important step towards large-scale preparation of well aligned perovskite nanowires for applications in high-density optoelectronic devices and on-chip integrated photonics systems.

For the growth of the directional perovskite nanowires, a mixture of CsBr and PbBr₂ powders (molar ratio 2:1) were firstly placed at the center of a heating zone of a quartz tube. Before the growth, several annealed M-plane sapphire sheets with aligned V-shaped nanogrooves at the surface were placed at the downstream as the growth substrates. At the same time high-purity N₂ gas was introduced into the quartz tube with a constant flowing rate (60 sccm). During the growth, the furnace was rapidly heated to 600 °C and maintained at this temperature for 10 min, with the pressure inside the tube kept at ~760 Torr (normal pressure). Then the furnace is naturally cooled down to room temperature. A large number of directional and ultra-long nanowires on the sapphire surface were obtained after the growth.

Figure 1a shows the typical low-magnification scanning electron microscope (SEM) image of the collected sample, which exhibits a large area of perfectly aligned CsPbBr₃ nanowires, with their length reaching up to several millimeters. The inset shows the corresponding SEM image of the annealed M-plane sapphire before growth, from which nanogrooves along the [1-210] direction could be clearly observed. The local high-magnification SEM images (Figures 1b, 1c, and S1) of the nanowires further demonstrate the ultra-smooth surface and perfect alignment of the as-grown nanowires, owning a well-defined triangular cross-section with the lateral size of 200 to 800 nm. In addition, the wires is well aligned along the observed nanogrooves at the surface of the sapphire substrate, indicating the nanogroove initiated growth of the nanowires (Figure S2).²³

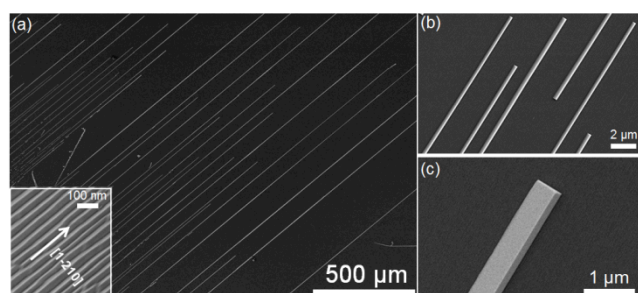


Figure 1. SEM images of the directional CsPbBr₃ nanowires growth along faceted M-plane sapphire. (a) Low-magnification SEM image of the ultra-long and directional CsPbBr₃ nanowires. Inset: SEM image of the annealed M-plane sapphire substrate with V-shaped nanogrooves along [1-210] direction. (b,c) High-magnification SEM images of CsPbBr₃ nanowires.

In order to investigate the crystal structure and growth mechanism of the directional CsPbBr₃ perovskite nanowires, we implemented the X-ray diffraction (XRD) and transmission electron microscopy (TEM) characterizations. As shown in Figure 2a, all the sharp diffraction peaks of the nanowires can be indexed to the monoclinic perovskite phase of CsPbBr₃.^{37,38} For the TEM measurements, a CsPbBr₃ nanowire was cut perpendicular to its length direction by a focused ion beam (FIB) system. The typical cross-sectional TEM image of the wire in Figure 2b indicates that the nanowire was tightly grown on the annealed M-plane sapphire, with several V-shape facets clearly exhibited at the nanowire-substrate interface region. Figure 2c shows the high-resolution TEM (HRTEM) image taken from the blue boxed region in Figure 2b, which displays clearly the graphoepitaxial relationship between nanowire and V-shaped nanogroove.²³ In addition, the measured lattice spacings of the nanowire are approximately 0.59 nm and 0.58 nm, corresponding to the (001) and (010) lattice plane of monoclinic perovskite CsPbBr₃.³⁸ The corresponding fast Fourier transform (FFT) pattern shows clear diffraction spots from both the substrate (red) and CsPbBr₃ nanowire (cyan), further demonstrating that the achieved directional nanowire is high-

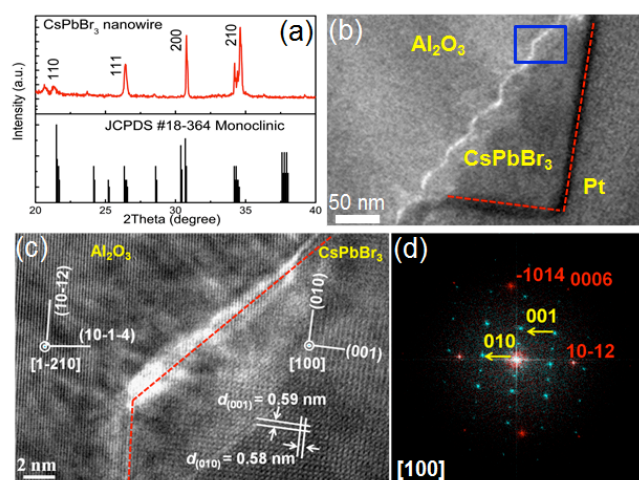


Figure 2. Microstructure characterizations of the directional CsPbBr₃ nanowires. (a) XRD pattern of the as-grown perovskite nanowires. (b) Cross-sectional TEM image of a perovskite nanowire. (c) HRTEM image recorded from the blue box marked area in (b). (d) The corresponding fast Fourier transform pattern at the interface.

crystallinity structure with the axial growth along [100] direction (Figure 2d).¹⁹ In addition, the formed nanowire with triangular cross-section is also thermodynamically favorable by exposing the (100) surfaces with low surface energy.^{19,33} The above SEM, XRD, and TEM results well demonstrate that the directional and ultra-long CsPbBr₃ nanowires with high-quality have been successfully achieved along the nanogrooves on the annealed M-plane sapphire.

The formation of these directional and ultra-long CsPbBr₃ nanowires can be understood from the following aspects. The vapor precursors firstly deposit and graphoepitaxially nucleate at the V-shaped nanogrooves of the sapphire substrate, as that revealed by the HRTEM in Figure 2c,²³ to form CsPbBr₃ nanocrystal seeds, which will further grow into one dimensional nanostructures along (100) planes with low surface energy.^{19,33} Benefiting from the existence of the nanogrooves, the nanowire growth can be realized directionally with [100] orientation along the V-shaped nanogrooves via graphoepitaxial effect driven by the maximum interface area between the substrate and nanowire as described previously.²³⁻²⁷ This is quite different from the observed orientation random growth of micro/nanorods on SiO₂/Si substrate.¹⁹ At the same time, it is interesting to find that a high growth pressure play a key role in realizing the ultra-long growth of the directional CsPbBr₃ nanowires. Comparison experiments at low pressure (~300 Torr) demonstrate that only microwires with larger diameter (2-5 μm) can be obtained, with their ultimate length less than hundred micrometer (Figure S3), greatly different from the achieved ultra-long (several millimeters) nanowires with small diameters at high pressure (760 Torr) (Figures 1 and S1). This may be explained since low pressure is more beneficial to the evaporation of source materials as compared to the high pressure growth, and results in the formation of microcrystals with a larger size at the initial growth stage (Figure S4).^{39,40} During the growth of these microcrystals into microwires, the graphoepitaxial effect induced axial growth could be greatly weakened compared to the high pressure nanowire growth, owing to their relatively smaller interface area between the substrate and the microwires, induced by their smaller surface-to-volume ratio. As a result, through tuning the growth pressure, directional and ultra-long CsPbBr₃ nanowires were successfully obtained on the annealed M-plane sapphires.

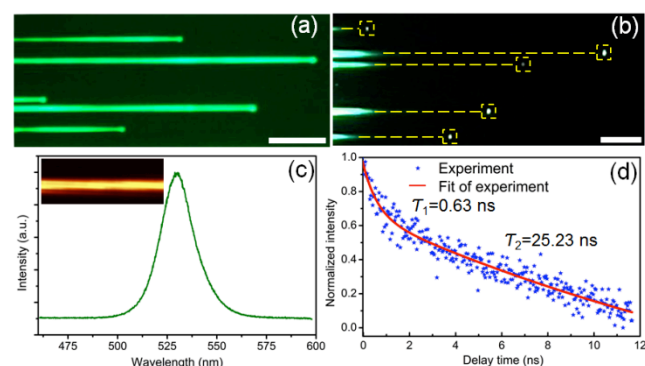


Figure 3. Optical characterizations of the ultra-long CsPbBr₃ nanowires. (a) Real-color photograph of the directional perovskite nanowires under diffused 405 nm laser illumination. Scale bar: 10 μm. (b) Aligned waveguide photograph with local excitation at the left of the nanowires. Scale bar: 10 μm. (c) PL spectrum of the nanowire. Inset: PL mapping of the nanowire. (d) Time-resolved PL (TRPL) decay kinetic after photoexcitation.

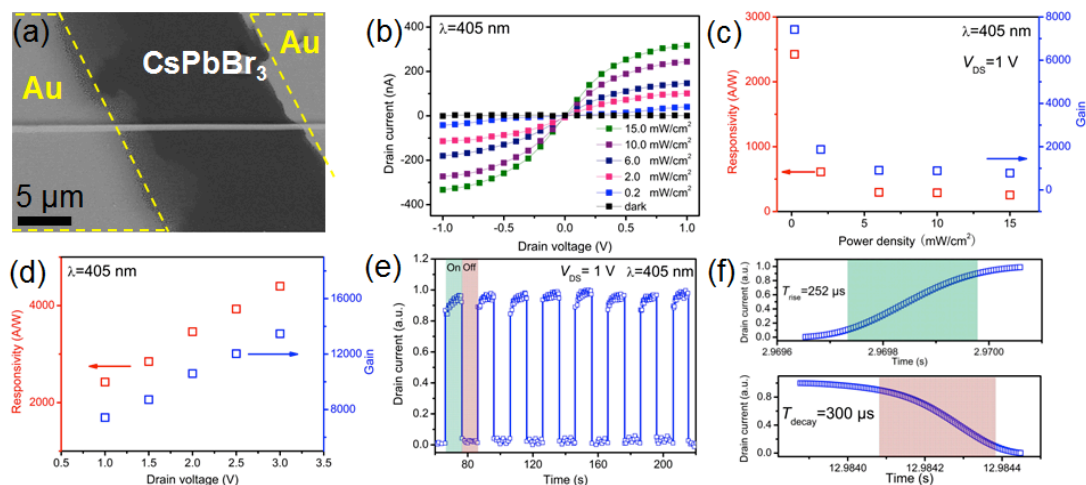


Figure 4. Optoelectronic characterizations of the directional CsPbBr₃ perovskite nanowires. (a) SEM image of the as-fabricated device. (b) I - V curves of the device measured at room temperature in the dark and under illumination with 405 nm light of different intensities. (c) Responsivity and gain vs. light intensity plot at a bias of 1 V. (d) Responsivity and gain as a function of the bias voltage (irradiance 0.2 mW/cm²). (e) The time-resolved response of the device under alternating dark and light illumination (10 mW/cm², 405 nm). The drain voltage is 1 V. (f) The rise (top) and decay (bottom) times of the photodetector.

Optical emission behaviors of the as-grown directional and ultra-long CsPbBr₃ nanowires were examined at the room temperature. Figure 3a is the real-color optical image of the as-grown nanowires under the broad illumination of a continuous-wave (CW) laser. Strong and uniform emission can be observed along the whole nanowire, demonstrating the high crystallinity of the nanowires. Figure 3b shows the optical waveguide photograph of the aligned CsPbBr₃ nanowires under a local excitation. The bright emission spots can be clearly seen at right tips of the nanowires, indicating the as-grown directional nanowires can form high-quality optical waveguide cavities. Figure 3c gives the normalized PL spectrum of CsPbBr₃ nanowire with a strong band edge emission peak at ~530 nm. The PL mapping in the inset also demonstrates the uniform PL emission along the wire. The charge carrier lifetimes were measured to estimate carrier dynamics in the aligned nanowires (The measurement details were shown in supporting information). As shown in Figure 3d, the PL decay curve was fitted by a biexponential profile, showing the long PL lifetime with $\tau_1=0.63$ and $\tau_2=25.23$ ns.^{41,42} The above optical characterizations demonstrate the superior optical capabilities and high crystallinity of the ultra-long perovskite nanowires, which help to realize high performance optoelectronic devices.

The photoelectronic characteristics of the CsPbBr₃ nanowires were investigated by fabricating devices based on an individual wire. The SEM image of the as-fabricated device is represented in Figure 4a. As shown, two Au (55 nm) electrodes were deposited on the nanowire. The width of the nanowire and the gap between the two electrodes are about 0.5 and 16.5 μ m, respectively. The current-voltage (I - V) curves of the device have been measured in the dark and under illumination with 405 nm light at different power intensities, as shown in Figure 4b. It can be observed that the photocurrent is proportional to the drain voltage and the illumination intensity. The photoresponsivity and gain are important parameters of photodetectors. The photoresponsivity of the nanowire detector can be expressed by I_{ph}/PS , where I_{ph} is the photocurrent, P is the incident power density irradiated on the nanowire, and S is the effective irradiated area on the wire.^{43,44}

The photoconductive gain can be expressed as $G=(I_{ph}/e)/(PS/h\nu)$, where I_{ph} is the photocurrent, P is the incident power density, S is

the effective irradiated area on the wire, $h\nu$ is the energy of an incident photon, and e is the electronic charge.⁴⁴ Figure 4c gives

the illumination power-dependent responsivity and gain of the device, demonstrating the high responsivity of 2.4×10^3 A/W and a high gain of 7.4×10^3 . We plot the responsivity and gain as a function of the bias as shown in Figure 4d. The detector shows significant performance at drain voltage of 3 V with responsivity of 4.4×10^3 A/W and gain of 1.3×10^4 , which are higher by one to six orders than the previously reported photodetectors based on single halide perovskite nano/microstructures.²⁸⁻³⁶ The wavelength dependent responsivity is also shown in Figure S5, demonstrating the high photoresponse under the light illumination with energy higher than the bandgap.⁴⁵

Fast response to optical signals is critical for optoelectronic applications of a photodetector. Figure 4e shows the response of photocurrent to optical pulses at a time interval of 10 s. We find that the dynamic photoresponse of the CsPbBr₃ photodetector is highly stable, indicating that the devices possess a remarkable photoswitching behavior. Figure 4f shows the temporal photoresponse of the photodetector. The rise and decay times of the photocurrent are 252 and 300 μ s, respectively, faster by one to three orders than the previous photodetectors based on single halide perovskite nano/microstructures.²⁸⁻³⁶ The exhibited high-performance of the photodetection as compared to previous single halide perovskite nano/microstructures (e.g. nanoplatelet, nanowire, nanosheet, and so on) can be attributed to the formation of high quality nanowire cavities without optical scattering and leakage from the surface, which helps to enhance the light absorption and confinement within the nanowires.^{14,46}

In summary, directional and ultra-long CsPbBr₃ perovskite nanowires were successfully synthesized on annealed M-plane sapphire substrates by a controlled vapor growth approach. The length of the achieved nanowires can reach up to several millimeters. The as-grown nanowires with high crystallinity own strong band edge emission and can act as excellent waveguide cavities. Photodetectors constructed based on the high-quality nanowires show prominent capabilities, with an ultra-high responsivity (4400 A/W) and a highly-fast response speed (252 μ s), which are much higher than all the previously reported photodetectors based on single halide perovskite nano/microstructures. This study demonstrates a new feasible method for directional growth of

large area ultra-long halide perovskite nanowires, which could find important applications in chip-scale integrated photonics and optoelectronic systems.

ASSOCIATED CONTENT

Supporting Information

The experiment details, SEM results, and wavelength dependent responsivity. This material is available free of charge via the Internet at <http://pubs.acs.org>

AUTHOR INFORMATION

Corresponding Author

*anlian.pan@hnu.edu.cn

Author Contributions

§ These authors contributed equally.

Notes

The authors declare no competing financial interests.

ACKNOWLEDGMENT

All authors are grateful to the NSF of China (Nos. 51525202, 61574054, 61505051, 51772088 and 61474040), the Hunan province science and technology plan (Nos. 2014FJ2001 and 2014TT1004), the Aid program for Science and Technology Innovative Research Team in Higher Educational Institutions of Hunan Province and the Fundamental Research Funds for the Central Universities. The Natural Science Foundation of Hunan Province (No. 2017JJ2025).

REFERENCES

- (1) Li, J.; Xu, L.; Wang, T.; Song, J.; Chen, J.; Xue, J.; Dong, Y.; Cai, B.; Shan, Q.; Han, B.; Zeng, H. *Adv. Mater.* 2017, 29, 1603885.
- (2) Dursun, I.; Shen, C.; Parida, M.; Pan, J.; Sarmah, S.; Priante, D.; Alyami, N.; Liu, J.; Saidaminov, M.; Alias, M.; Abdelhady, A.; Ng, Tien, Mohammed, O.; Ooi, B.; Bakr, O. *ACS Photonics* 2016, 3, 1150.
- (3) Zhu, H.; Fu, Y.; Meng, F.; Wu, X.; Gong, Z.; Ding, Q.; Gustafsson, M.; Trinh, M.; Jin, S.; Zhu, X. *Nat. Mater.* 2015, 14, 636.
- (4) Waleed, A.; Tavakoli, M.; Gu, L.; Hussain, S.; Zhang, D.; Poddar, S.; Wang, Z.; Zhang, R.; Fan, Z. *Nano Lett.* 2017, 17, 4951.
- (5) Min, X.; Zhu, P.; Gu, S.; Zhu, J. *J. Semicond.* 2017, 38, 011004.
- (6) Quan, L.; Quintero-Bermudez, R.; Voznyy, O.; Walters, G.; Jain, A.; Fan, J.; Zheng, X.; Yang, Z.; Sargent, E. *Adv. Mater.* 2017, 29, 1605945.
- (7) Zhang, J.; Yang, X.; Deng, H.; Qiao, K.; Farooq, U.; Ishaq, M.; Yi, F.; Liu, H.; Tang, J.; Song, H. *Nano-Micro Lett.* 2017, 9, 36.
- (8) Zhang, Q.; Su, R.; Du, W.; Liu, X.; Zhao, L.; Ha, S.; Xiong, Q. *Small Methods* 2017, 1, 1700163.
- (9) Zhang, D.; Yu, Y.; Bekenstein, Y.; Wong, A. B.; Alivisatos, A. P.; Yang, P. D. *J. Am. Chem. Soc.* 2016, 138, 13155.
- (10) Zhang, D.; Eaton, S. W.; Yu, Y.; Dou, L. T.; Yang, P. D. *J. Am. Chem. Soc.* 2015, 137, 9230.
- (11) Bekenstein, Y.; Koscher, B. A.; Eaton, S. W.; Yang, P. D.; Alivisatos, A. P. *J. Am. Chem. Soc.* 2015, 137, 16008.
- (12) Hu, X.; Zhou, H.; Jiang, Z.; Wang, X.; Yuan, S.; Lan, J.; Fu, Y.; Zhang, X.; Zheng, W.; Wang, X.; Zhu, X.; Liao, L.; Xu, G.; Jin, S.; Pan, A. *ACS Nano* 2017. DOI: 10.1021/acsnano.7b03660
- (13) Zhang, Q.; Su, R.; Liu, X.; Xing, J.; Sum, T. C.; Xiong, Q.; *Adv. Funct. Mater.* 2016, 26, 6238.
- (14) Wang, Y.; Sun, X.; Shivanna, R.; Yang, Y.; Chen, Z.; Guo, Y.; Wang, G.; Wertz, F.; Deschler, F.; Cai, Z.; Zhou, H.; Lu, T.; Shi, J. *Nano Lett.* 2016, 16, 7974.
- (15) Chen, J.; Fu, Y.; Samad, L.; Dang, L.; Zhao, Y.; Shen, S.; Guo, L.; Jin, S. *Nano Lett.* 2017, 17, 460.
- (16) Zhou, H.; Yuan, S.; Wang, X.; Xu, T.; Wang, X.; Li, H.; Zheng, W.; Fan, P.; Li, Y.; Sun, L.; Pan, A. *ACS Nano* 2017, 11, 1189.
- (17) Wang, X.; Yuan, S.; Zheng, W.; Zhou, H.; Jiang, Y.; Zhuang, X.; Liu, H.; Zhang, Q.; Zhu, X.; Wang, X.; Pan, A. *Nano Res.* 2017, 10, 3385.
- (18) Liu, Z.; Jiao, L.; Yao, Y.; Xian, X.; Zhang, J. *Adv. Mater.* 2010, 22, 2285.
- (19) Zhang, Y.; Wang, X.; Wu, Y.; Jie, J.; Zhang, X.; Xing, Y.; Wu, H.; Zou, B.; Zhang, X.; Zhang, X. *J. Mater. Chem.* 2012, 22, 14357.
- (20) Yao, J.; Yan, H.; Lieber, C. *Nat. Nanotechnol.* 2013, 8, 329.
- (21) Deng, W.; Zhang, X.; Huang, L.; Xu, X.; Wang, L.; Wang, J.; Shang, Q.; Lee, S.; Jie, J. *Adv. Mater.* 2016, 28, 2201.
- (22) Chen, J.; Morrow, D.; Fu, Y.; Zheng, W.; Zhao, Y.; Dang, L.; Stolt, M.; Kohler, D.; Wang, X.; Czech, K.; Hautzinger, M.; Shen, S.; Guo, L.; Pan, A.; Wright, J.; Jin, S. *J. Am. Chem. Soc.* 2017, 139, 13525.
- (23) Tsvivion, D.; Schwartzman, M.; Popovitz-Biro, R.; Huth, P.; Joselevich, E. *Science.* 2011, 333, 1003.
- (24) Shalev, E.; Oksenberg, E.; Rechav, K.; Popovitz-Biro, R.; Joselevich, E. *ACS Nano* 2017, 11, 213.
- (25) Oksenberg, E.; Popovitz-Biro, R.; Rechav, K.; Joselevich, E. *Adv. Mater.* 2015, 27, 3999.
- (26) Oksenberg, E.; Martí-Sánchez, S.; Popovitz-Biro, R.; Arbiol, J.; Joselevich, E. *ACS Nano* 2017, 11, 6155.
- (27) Wang, X.; Aroonyadet, N.; Zhang, Y.; Mecklenburg, M.; Fang, X.; Chen, H.; Goo, E.; Zhou, C. *Nano Lett.* 2014, 6, 3014.
- (28) Niu, L.; Zeng, Q.; Shi, J.; Cong, C.; Wu, C.; Liu, F.; Zhou, J.; Fu, W.; Fu, Q.; Jin, C.; Yu, T.; Liu, X.; Liu, Z. *Adv. Funct. Mater.* 2016, 26, 5263.
- (29) Zhuo, S.; Zhang, J.; Shi, Y.; Huang, Y.; Zhang, B. *Angew. Chem. Int. Ed.* 2015, 54, 5693.
- (30) Liu, J.; Xue, Y.; Wang, Z.; Xu, Z.; Zheng, C.; Weber, B.; Song, J.; Wang, Y.; Lu, Y.; Zhang, Y.; Bao, Q. *ACS Nano* 2016, 10, 3536.
- (31) Dong, D.; Deng, H.; Hu, C.; Song, H.; Qiao, K.; Yang, X.; Zhang, J.; Cai, F.; Tang, J.; Song, H. *Nanoscale* 2017, 9, 1567.
- (32) Li, P.; Shivananju, B.; Zhang, Y.; Li, S.; Bao, Q. *J. Phys. D: Appl. Phys.* 2017, 50, 094002.
- (33) Chen, J.; Fu, Y.; Samad, L.; Dang, L.; Shen, Z.; Guo, L.; Jin, S. *Nano Lett.* 2017, 17, 460.
- (34) Wang, S.; Wang, K.; Gu, Z.; Wang, Y.; Huang, C.; Yi, N.; Xiao, S.; Song, Q. *Adv. Opt. Mater.* 2017, 1700023.
- (35) Lai, M.; Kong, Q.; Bischak, C.; Yu, Y.; Dou, L.; Eaton, S.; Ginsberg, N.; Yang, P. *Nano Res.* 2017, 10, 1107.
- (36) Tang, X.; Zu, Z.; Shao, H.; Hu, W.; Zhou, M.; Deng, M.; Chen, W.; Zang, Z.; Zhu, T.; Xue, J. *Nanoscale* 2016, 8, 15158.
- (37) Wang, H.; Lin, S.; Tang, A.; Singh, B.; Tong, H.; Chen, Y.; Lee, Y.; Tsai, T.; Liu, R. *Angew. Chem. Int. Ed.* 2016, 55, 7924.
- (38) Song, Y.; Yoo, J.; Kang, B.; Choi, S.; Ji, E.; Jung, H.; Yoon, D. *Nanoscale* 2016, 8, 19523.
- (39) Dalal, S.; Baptista, D.; Teo, K.; Lacerda, R.; Jefferson, D.; Milne, W. *Nanotechnology* 2006, 17, 4811.
- (40) Li, S.; Zhang, X.; Yan, B.; Yu, T. *Nanotechnology* 2009, 20, 495604.
- (41) Zhang, Q.; Wang, S.; Liu, X.; Chen, T.; Li, H.; Liang, J.; Zheng, W.; Agarwal, R.; Lu, W.; Pan, A. *Nano Energy* 2016, 30, 481.
- (42) Zhang, Q.; Liu, H.; Guo, P.; Li, D.; Fan, P.; Zheng, W.; Zhu, X.; Jiang, Y.; Zhou, H.; Hu, W.; Zhuang, X.; Liu, H.; Duan, X.; Pan, A. *Nano Energy* 2017, 32, 28.
- (43) Zhang, X.; Yang, S.; Zhou, H.; Liang, J.; Liu, H.; Xia, H.; Zhu, X.; Jiang, Y.; Zhang, Q.; Hu, W.; Zhuang, X.; Liu, H.; Hu, W.; Wang, X.; Pan, A. *Adv. Mater.* 2017, 29, 1604431.
- (44) Zheng, D.; Wang, J.; Hu, W.; Liao, L.; Fang, H.; Guo, N.; Wang, P.; Gong, F.; Wang, X.; Fan, Z.; Wu, X.; Meng, X.; Chen, X.; Lu, W. *Nano Lett.* 2016, 16, 2548.
- (45) Zhu, P.; Gu, S.; Shen, X.; Xu, N.; Tan, Y.; Zhuang, S.; Deng, Y.; Lu, Z.; Wang, Z.; Zhu, J. *Nano Lett.* 2016, 16, 871.
- (46) Peng, M.; Yu, X.; Cai, X.; Yang, Q.; Hu, H.; Yan, K.; Wang, H.; Dong, B.; Zhu, F.; Zou, D. *Nano Energy* 2014, 10, 117.

